

# CrossMPT: Cross-attention Message-Passing Transformer for Error Correcting Codes

Seong-Joon Park<sup>1</sup> Hee-Youl Kwak<sup>2</sup> Sang-Hyo Kim<sup>3</sup> Yongjune Kim<sup>4</sup> Jong-Seon No<sup>5</sup>

## Abstract

Error correcting codes (ECCs) are indispensable for reliable transmission in communication systems. The recent advancements in deep learning have catalyzed the exploration of ECC decoders based on neural networks. Among these, transformer-based neural decoders have achieved state-of-the-art decoding performance. In this paper, we propose a novel Cross-attention Message-Passing Transformer (CrossMPT). CrossMPT iteratively updates two types of input vectors (i.e., magnitude and syndrome vectors) using two masked cross-attention blocks. The mask matrices in these cross-attention blocks are determined by the code's parity-check matrix that delineates the relationship between magnitude and syndrome vectors. Our experimental results show that CrossMPT significantly outperforms existing neural network-based decoders, particularly in decoding low-density parity-check codes. Notably, CrossMPT also achieves a significant reduction in computational complexity, achieving over a 50% decrease in its attention layers compared to the original transformer-based decoder, while retaining the computational complexity of the remaining layers.

## 1. Introduction

The fundamental objective of digital communication systems is to ensure the reliable transmission of information from source to destination through noisy channels. Error correcting codes (ECCs) are crucial for ensuring the integrity

of transmitted data in digital communication systems. The advancements in deep learning across diverse tasks, such as natural language processing (NLP) (Devlin et al., 2019; Brown et al., 2020), image classification (Krizhevsky et al., 2012; Simonyan & Zisserman, 2015; Szegedy et al., 2015; He et al., 2016), and object detection (Girshick et al., 2014; Ren et al., 2015; He et al., 2015; Redmon et al., 2015; Carion et al., 2020), have motivated the application of deep learning techniques to ECC decoders. This has led to the development of neural decoders (Kim et al., 2018; 2020; Nachmani et al., 2016; 2018; Dai et al., 2021; Lugosch & Gross, 2017). The key aim of these neural decoders is to improve decoding performance by overcoming limitations of the conventional decoders such as belief propagation (BP) (Richardson & Urbanke, 2001) or min-sum (MS) (Fossorier et al., 1999) decoders.

Among neural decoders, a model-free neural decoder employs an arbitrary neural network architecture as the ECC decoder itself without relying on prior knowledge of specific decoding algorithms. To circumvent overfitting problems, these neural decoders incorporate a preprocessing step where the magnitude and syndrome vectors from the received codeword are concatenated and then utilized as inputs. This preprocessing enables decoders to learn the channel noise effectively by resolving overfitting (Bennatan et al., 2018). This approach significantly improves the decoding performance of model-free neural decoders (Choukroun & Wolf, 2022a; 2023; Park et al., 2023). However, it raises two important questions: 1) how to handle these two distinct types of input vectors efficiently, and 2) how to design the optimal decoder architectures.

Recent transformer-based ECC decoders (Choukroun & Wolf, 2022a; 2023; Park et al., 2023) adopt the concatenation of the magnitude and syndrome vectors as a single input vector and utilize the masked self-attention blocks to learn the channel noise. In these blocks, a mask matrix derived from the parity check matrix (PCM) is employed to facilitate the training process by considering the relationship between the combined magnitude and syndrome vectors.

In contrast, our approach separates the magnitude and syndrome vectors by recognizing their distinct informational characteristics. The *real-valued* magnitude vector indicates

<sup>1</sup>Institute of Artificial Intelligence, Pohang University of Science and Technology (POSTECH) <sup>2</sup>School of Electrical Engineering, University of Ulsan <sup>3</sup>Department of Electrical and Computer Engineering, Sungkyunkwan University <sup>4</sup>Department of Electrical Engineering, Pohang University of Science and Technology (POSTECH) <sup>5</sup>Department of Electrical and Computer Engineering, Seoul National University. Correspondence to: Hee-Youl Kwak <hykwak@ulsan.ac.kr>, Yongjune Kim <yongjune@postech.ac.kr>.

the reliability of each bit position, whereas the *binary* syndrome vector conveys the information of bit error positions. This deliberate separation necessitates the development of a novel architecture of transformer-based decoder, specifically designed to effectively handle these separated magnitude and syndrome vectors, thereby significantly improving decoding performance.

In this paper, we introduce a novel Cross-attention Message-Passing Transformer (CrossMPT) for ECC decoding. CrossMPT processes the magnitude and syndrome vectors separately without concatenation to effectively utilize their distinct informational properties. It employs two *masked cross-attention blocks* to iteratively update the magnitude and syndrome vectors. Initially, the magnitude vector is encoded into the *query*, while the syndrome vector is encoded into *key* and *value*. The first cross-attention block utilizes this configuration in its attention mechanism to update the magnitude vector's component. This procedure is reciprocated for the syndrome vector, encoded into the query, while the magnitude vector is encoded into key and value. This configuration enables the second cross-attention block to update the syndrome vector component effectively. These two masked cross-attention blocks iteratively collaborate to refine the magnitude and syndrome vectors as in the message-passing algorithm (Richardson & Urbanke, 2001).

To facilitate the training, CrossMPT employs two mask matrices: the PCM  $H$  and its transpose  $H^T$ . This strategy is supported by the PCM's inherent representation of the 'magnitude-syndrome' relationship, effectively aligning with the architecture's objectives. To our knowledge, CrossMPT is the first architecture to integrate an iterative message-passing framework with a cross-attention-based transformer architecture.

Experimental results show that CrossMPT outperforms the original ECCT across various code types, with notable improvement in decoding low-density parity-check (LDPC) codes. Beyond enhanced decoding performance, CrossMPT achieves a significant reduction in the computational complexity of the attention module by over 50% compared to the original ECCT, while the complexity of other layers remains unchanged. Considering the attention module's substantial portion of the total computational complexity, this reduction leads to a significant decrease in overall computational complexity.

## 2. Background

### 2.1. Error Correcting Codes

Let  $C$  be a linear block code, which can be defined by a generator matrix  $G$  of size  $k \times n$  and a parity check matrix  $H$  of size  $(n - k) \times n$ , which satisfy  $GH^T = 0$  over  $\{0, 1\}$  with modulo 2 addition. A codeword  $x \in C \subset \{0, 1\}^n$  can

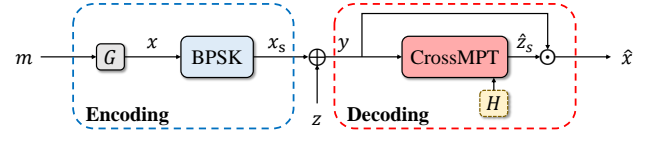


Figure 1. A brief model of a digital communication system with CrossMPT.

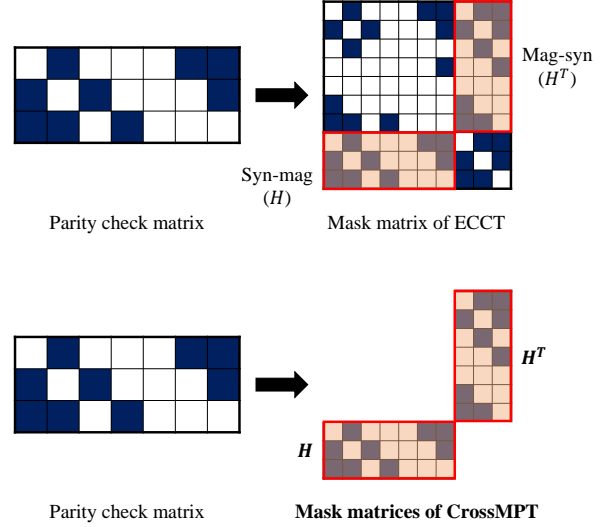


Figure 2. The PCM and the mask matrices of ECCT (Choukroun & Wolf, 2022a) and CrossMPT.

be encoded by multiplying message  $m$  with the generator matrix  $G$  (i.e.,  $x = mG$ ). Let  $x_s$  be the BPSK modulated version for  $x$  (e.g., for binary phase shift keying modulation,  $x_s = +1$  if  $x = 0$  and  $x_s = -1$  if  $x = 1$ ) and let  $y$  be the output of a noisy channel for input  $x_s$  (see Figure 1). We assume the additive white Gaussian noise (AWGN) channel and the channel output can be defined by  $y = x_s + z$ , where  $z \sim N(0, \sigma^2)$ . The objective of the decoder ( $f: \mathbb{R}^n \rightarrow \mathbb{R}^n$ ) is to recover the original transmitted codeword  $x$  by correcting errors. When  $y$  is received, the decoder first determines whether the received signal is corrupted or not by checking the syndrome  $s(y) = Hy_b$ , where  $y_b = \text{bin}(\text{sign}(y))$  is a signal after the demodulation of  $y$ . Here,  $\text{sign}(a)$  represents  $+1$  if  $a \geq 0$  and  $-1$  otherwise and  $\text{bin}(-1) = 1$ ,  $\text{bin}(+1) = 0$ . If  $s(y)$  is a non-zero vector, it is detected that  $y$  is corrupted during the transmission, and the decoder initiates the error correction process.

### 2.2. Error Correction Code Transformer

Error correction code transformer (ECCT) is the first work to present a model-free ECC decoder with the transformer

architecture. ECCT outperforms other neural BP-based decoders by employing the masked self-attention mechanism, whose mask matrix is determined by the code's PCM (Choukroun & Wolf, 2022a). Based on the preprocessing method in (Bennatan et al., 2018), ECCT utilizes the magnitude and syndrome vectors to train multiplicative noise  $\tilde{z}_s$ , which is defined by

$$y = x_s + z = x_s \tilde{z}_s. \quad (1)$$

The preprocessing method resolves the overfitting problem in the model-free neural decoder and enables to learn the multiplicative noise with the all-zero codeword.

ECCT aims to estimate the multiplicative noise in (1). Thus,  $f(y) = \hat{z}_s$  and the estimation of  $x$  is  $\hat{x} = \text{bin}(\text{sign}(yf(y)))$ . If the multiplicative noise is correctly estimated, then  $\text{sign}(\hat{z}_s) = \text{sign}(z_s)$  and  $\text{sign}(\hat{z}_s \hat{z}_s) = 1$ . In this case,  $\hat{x}$  is obtained by

$$\begin{aligned} \hat{x} &= \text{bin}(\text{sign}(yf(y))) = \text{bin}(\text{sign}(x_s \tilde{z}_s \hat{z}_s)) \\ &= \text{bin}(\text{sign}(x_s)) = x. \end{aligned}$$

ECCT employs a masked self-attention module to train the transformer architecture, where the input embedded vector is the concatenation of the magnitude and syndrome vector of  $y$ .

A key property of ECCT is that the mask matrix for the attention module is constructed based on the PCM, enabling the mask matrix to encapsulate information about the relationship between codeword bits. As shown in Figure 2, the mask matrix of ECCT contains all relationships between magnitude itself, magnitude and syndrome, and the syndrome itself.

However, the proposed CrossMPT utilizes only mask matrices that represent the relationship between magnitude and syndrome, which leads to the adoption of a masked cross-attention module. Two red squares in Figure 2 represent the PCM  $H$  (syndrome-magnitude relationship) and its transpose  $H^T$  (magnitude-syndrome relationship), which are the mask matrices of two masked cross-attention modules in CrossMPT as presented in Section 3.

### 3. Cross-attention Message-passing Transformer (CrossMPT)

In this section, we present the cross-attention message-passing transformer called CrossMPT. In CrossMPT, the magnitude and syndrome vectors of the received codeword iteratively update each other, thereby improving the decoding performance. The overall architecture is depicted in Figure 3.

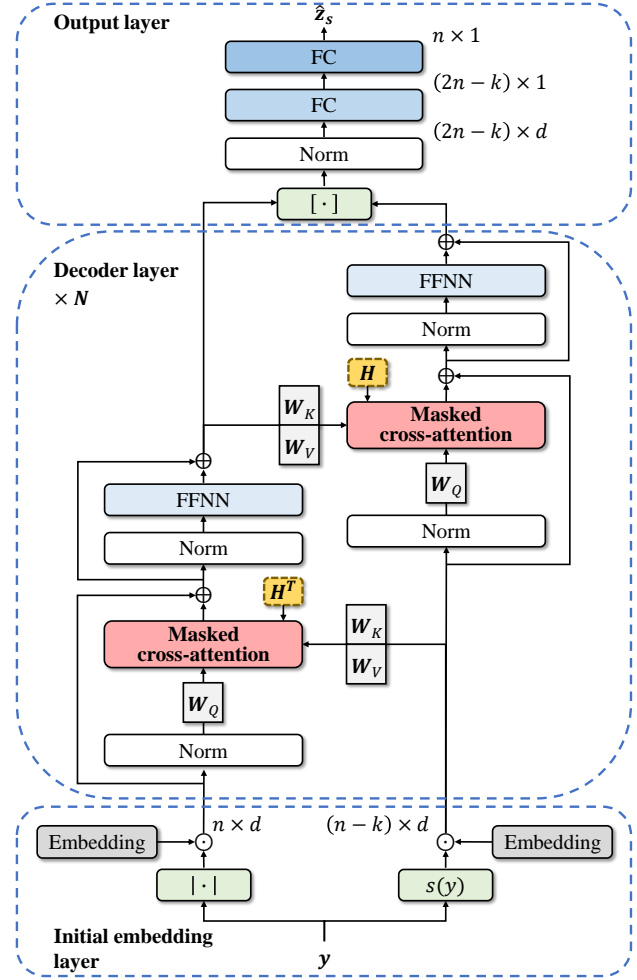


Figure 3. Architecture of CrossMPT.

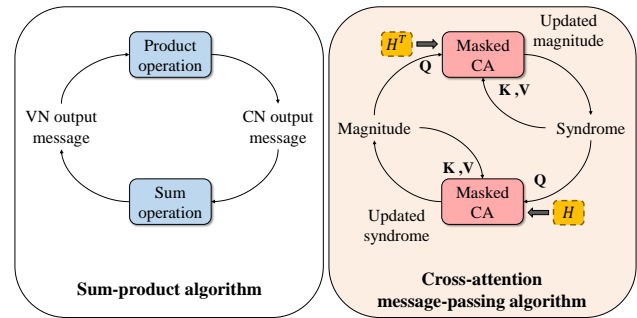


Figure 4. Conceptual comparison of the sum-product algorithm and the proposed cross-attention (CA) message passing algorithm.

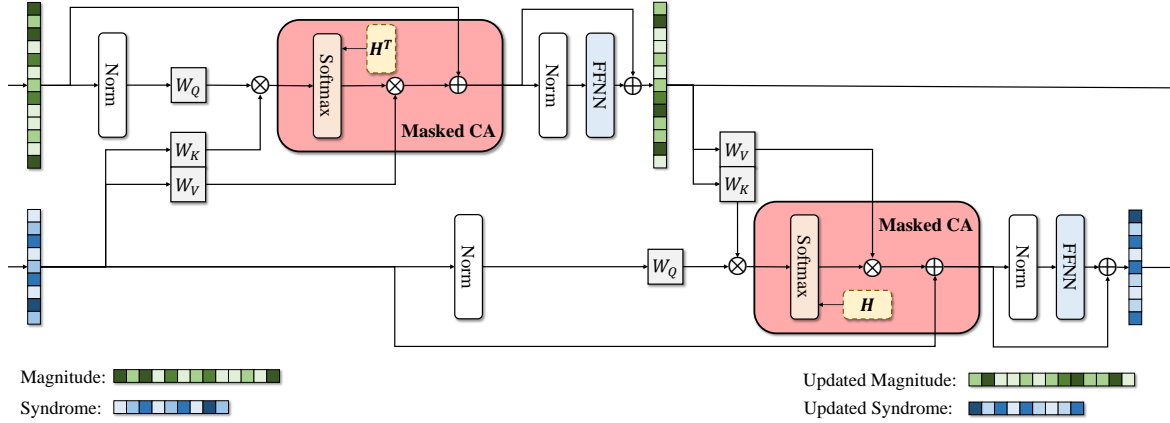


Figure 5. Cross-attention module for CrossMPT.

### 3.1. Cross-attention Message-passing Algorithm with Magnitude and Syndrome

The message passing algorithms such as the sum-product algorithm (Richardson & Urbanke, 2001) are widely used for decoding ECCs due to their outstanding decoding performance with low complexity. The sum-product decoder operates by exchanging messages between variable nodes (VNs) and check nodes (CNs) in a Tanner (bipartite) graph (Richardson & Urbanke, 2001). In the Tanner graph, VNs convey information about the reliability of the received codeword, while CNs indicate the parity check equations. The edges between VNs and CNs represent the connections (relationships) between them. The message-passing decoder operates by exchanging messages between VNs and CNs via edges. The output messages of VNs and CNs are updated in an iterative manner.

Inspired by the principles of message-passing algorithms, CrossMPT exchanges messages between the magnitude vector  $|y|$  and the syndrome vector  $s(y)$ . Initially, we update the  $|y|$  by the masked cross-attention block, with  $|y|$  as the query and  $s(y)$  as both key and value. Given this configuration, the attention map has the size  $n \times (n - k)$ , effectively representing the ‘magnitude-syndrome’ relation. To reflect this relationship, we employ the transpose of the PCM  $H^T$  as the mask matrix. This is because the  $n$  rows of  $H^T$  correspond to the  $n$  bit positions, and its  $n - k$  columns are associated with the parity check equations, directly linking to  $|y|$  and  $s(y)$ , respectively. The outcome of this process is an updated magnitude.

The syndrome  $s(y)$  is updated in the subsequent masked cross-attention block, utilizing the previously updated magnitude. In this block,  $s(y)$  is used as the query, while the updated  $|y|$  serves as both key and value. For this operation, we utilize the parity check matrix (PCM)  $H$  as the mask ma-

trix. The resulting output from this cross-attention block is the updated syndrome. CrossMPT iteratively updates both the magnitude and syndrome to identify the multiplicative noise accurately.

As a representative of the message-passing algorithm, Figure 4 depicts the sum-product algorithm and the cross-attention message-passing algorithm. In the sum-product algorithm, the VN output and CN output messages are iteratively updated using the sum and product operations. Similar to the sum-product algorithm, the magnitude and syndrome vectors are iteratively updated using the masked cross-attention (Masked CA in the figure) blocks in CrossMPT. Note that  $H$  and  $H^T$  are utilized for the mask matrices for these cross-attention blocks, and  $Q$ ,  $K$ , and  $V$  represent the query, key, and value of the cross-attention mechanism.

### 3.2. Model Architecture

In the initial embedding layer of CrossMPT, we generate  $|y|$  and  $s(y)$ , which are the magnitude and syndrome vectors of  $y$ . Rather than concatenating  $|y|$  and  $s(y)$  as in the original ECCT (Choukroun & Wolf, 2022a; 2023; Park et al., 2023), each vector is considered a distinct input in CrossMPT. All the elements of the  $n$ -dimensional magnitude vector  $|y|$  and the  $(n - k)$ -dimensional syndrome vector  $s(y)$  are individually projected into  $d$  dimension embedding vectors.

These two embedded vectors are processed as separate input vectors in the following  $N$  decoding layers. As shown in Figures 3 and 5, each decoder layer consists of a cross-attention module, followed by a feed-forward neural network (FFNN), where a normalization layer precedes. In the decoder layer, we first update the  $|y|$  through the masked cross-attention block, in which  $|y|$  is set as the query and  $s(y)$  is set as both key and value. This configuration results in an attention map of size  $n \times (n - k)$ , representing the

‘magnitude-syndrome’ relationship. Therefore, we use the transpose of the PCM  $H^T$  as a mask matrix since the  $n$  rows of  $H^T$  correspond to  $n$  bit positions and the  $n - k$  columns of  $H^T$  to parity check equations, which are closely related to  $|y|$  and  $s(y)$ , respectively. Finally, the output vector embodies a newly updated magnitude vector by using the syndrome information.

Subsequently, the updated  $|y|$  is utilized to update  $s(y)$  in the subsequent masked cross-attention block. In this block,  $s(y)$  acts as the query, and the updated  $|y|$  serves as the key and value. Since the  $s(y)$  acts as a query, we use the PCM  $H$  as a mask matrix. Again, the output vector conveys the updated syndrome and is utilized to further refine the magnitude vector. This process is iteratively repeated during the  $N$  decoder layers.

Finally, these output vectors of the last decoder layer are concatenated and pass through a normalization layer and two fully connected (FC) layers. The first FC layer reduces the  $2n - k \times d$  dimension embedding to a one-dimensional  $2n - k$  vector, and the second FC layer further reduces the dimension from  $2n - k$  into  $n$ . The final output provides an estimation of  $\tilde{z}_s$ .

### 3.3. Training

The objective of the proposed decoder is to learn the multiplicative noise  $\tilde{z}_s$  in (1) and reconstruct the original transmitted signal  $x$ . We can obtain the multiplicative noise by  $\tilde{z}_s = \tilde{z}_s x_s^2 = y x_s$ . Then, the target multiplicative noise for binary cross-entropy loss function is defined by  $\tilde{z} = \text{bin}(\text{sign}(y x_s))$ . Finally, the cross-entropy loss function for a received codeword  $y$  is defined by

$$\mathcal{L} = - \sum_{i=1}^n \{ \tilde{z}_i \log(\sigma(f(y))) + (1 - \tilde{z}_i) \log(1 - \sigma(f(y))) \}.$$

To ensure a fair comparison between the CrossMPT and ECCT, we adopt the same training setup used in the previous work (Choukroun & Wolf, 2022a). We use the Adam optimizer (Kingma & Ba, 2014) and conduct 1000 epochs. Each epoch consists of 1000 minibatches, where each minibatch is composed of 128 samples. All simulations were conducted using NVIDIA GeForce RTX 3090 GPU and AMD Ryzen 9 5950X 16-Core Processor CPU.

The preprocessing step (Bennatan et al., 2018) enables the use of the all-zero codeword for training. The training sample  $y$  is generated by  $y = x_s + z$ , where the AWGN channel noise  $z$  is from SNR ( $E_b/N_0$ ) range of 3 dB to 7 dB. The learning rate is initially set to  $10^{-4}$  and gradually reduced to  $5 \times 10^{-7}$  following a cosine decay scheduler.

## 4. Performance Evaluation

To verify the efficacy of CrossMPT, we train CrossMPT for BCH codes, polar codes, and LDPC codes and evaluate the bit error rate (BER) performance. All PCMs are derived from (Helmling et al., 2019). The implementation of the original ECCT is taken from (Choukroun & Wolf, 2022b). For the testing, we collect at least 500 frame errors at each signal-to-noise ratio (SNR) value for at least  $10^5$  random codewords. Table 1 compares the decoding performance of CrossMPT with the BP decoder, BP-based neural decoders (Nachmani & Wolf, 2019; 2021), and ECCT (Choukroun & Wolf, 2022a). The results of the BP-based decoders in Table 1 are obtained after 50 BP iterations. The results for both the proposed CrossMPT and ECCT, which are model-free decoders, are obtained with  $N = 6$  and  $d = 128$ . For all types of codes, CrossMPT outperforms the ECCT and all the other BP-based neural decoders. This improvement of the CrossMPT is particularly notable in the case of polar and LDPC codes. To provide more visual information, we plot the BER graphs for several codes in Figure 6.

In Figure 7, present a comparison of the BER performance between the CrossMPT and ECCT for the (384, 320) wireless regional area network (WRAN) LDPC code as a representative example of a long code. Despite its reduced complexity, CrossMPT significantly enhances the decoding performance compared to ECCT, not only for short-length codes but also for long-length codes. The evaluation is conducted with  $N = 6$ ,  $d = 32$ , but since CrossMPT highly reduces the computational complexity compared to ECCT, the performance evaluation for larger codeword length and larger  $d$  would be possible.

## 5. Discussion

In this section, we compare the number of parameters and computational complexity of the CrossMPT and ECCT (Choukroun & Wolf, 2022a) to show the complexity reduction of the CrossMPT.

### 5.1. Number of Parameters

CrossMPT and the original ECCT models have the same number of parameters. In each decoder layer of CrossMPT, two cross-attention transformer blocks share the same parameters for normalization layer, masked cross-attention module, and FFNN layer. Also, for the output layer, two decoders have the same number of parameters in their two fully-connected (FC) layers.



Table 1. A comparison of decoding performance at three different SNR values (4 dB, 5 dB, 6 dB) for BP decoder, Hyper BP decoder (Nachmani & Wolf, 2019), AR BP decoder (Nachmani & Wolf, 2021), ECCT (Choukroun & Wolf, 2022a), and the proposed CrossMPT. The results are measured by the negative natural logarithm of BER. The best results are highlighted in **bold**. Higher is better.

Codes	Method	BP-based decoders									Model-free decoders					
		BP			Hyp BP			AR BP			ECCT			CrossMPT		
		4	5	6	4	5	6	4	5	6	4	5	6	4	5	6
BCH	(31,16)	4.63	5.88	7.60	5.05	6.64	8.80	5.48	7.37	9.60	6.39	8.29	10.66	<b>6.98</b>	<b>9.25</b>	<b>12.48</b>
	(63,36)	4.03	5.42	7.26	4.29	5.91	8.01	4.57	6.39	8.92	4.86	6.65	9.10	<b>5.03</b>	<b>6.91</b>	<b>9.37</b>
	(63,45)	4.36	5.55	7.26	4.64	6.27	8.51	4.97	6.90	9.41	5.60	7.79	10.93	<b>5.90</b>	<b>8.20</b>	<b>11.62</b>
	(63,51)	4.5	5.82	7.42	4.8	6.44	8.58	5.17	7.16	9.53	5.66	7.89	11.01	<b>5.78</b>	<b>8.08</b>	<b>11.41</b>
Polar	(64,32)	4.26	5.38	6.50	4.59	6.10	7.69	5.57	7.43	9.82	6.99	9.44	12.32	<b>7.50</b>	<b>9.97</b>	<b>13.31</b>
	(64,48)	4.74	5.94	7.42	4.92	6.44	8.39	5.41	7.19	9.30	6.36	8.46	11.09	<b>6.51</b>	<b>8.70</b>	<b>11.31</b>
	(128,64)	4.1	5.11	6.15	4.52	6.12	8.25	4.84	6.78	9.3	5.92	8.64	12.18	<b>7.52</b>	<b>11.21</b>	<b>14.76</b>
	(128,86)	4.49	5.65	6.97	4.95	6.84	9.28	5.39	7.37	10.13	6.31	9.01	12.45	<b>7.51</b>	<b>10.83</b>	<b>15.24</b>
	(128,96)	4.61	5.79	7.08	4.94	6.76	9.09	5.27	7.44	10.2	6.31	9.12	12.47	<b>7.15</b>	<b>10.15</b>	<b>13.13</b>
LDPC	(49,24)	6.23	8.19	11.72	6.23	8.54	11.95	6.58	9.39	12.39	6.13	8.71	12.10	<b>6.68</b>	<b>9.52</b>	<b>13.19</b>
	(121,60)	4.82	7.21	10.87	5.22	8.29	13.00	5.22	8.31	13.07	5.17	8.31	13.30	<b>5.74</b>	<b>9.26</b>	<b>14.78</b>
	(121,70)	5.88	8.76	13.04	6.39	9.81	14.04	6.45	10.01	14.77	6.40	10.21	16.11	<b>7.06</b>	<b>11.39</b>	<b>17.52</b>
	(121,80)	6.66	9.82	13.98	6.95	10.68	15.80	7.22	11.03	15.90	7.41	11.51	16.44	<b>7.99</b>	<b>12.75</b>	<b>18.15</b>
Mackay	(96,48)	6.84	9.40	12.57	7.19	10.02	13.16	7.43	10.65	14.65	7.38	10.72	14.83	<b>7.97</b>	<b>11.77</b>	<b>15.52</b>
CCSDS	(128,64)	6.55	9.65	13.78	6.99	10.57	15.27	7.25	10.99	16.36	6.88	10.90	15.90	<b>7.68</b>	<b>11.88</b>	<b>17.50</b>
Turbo	(132,40)	N/A	N/A	N/A	N/A	N/A	N/A	N/A	N/A	N/A	4.74	6.54	9.06	<b>5.55</b>	<b>7.92</b>	<b>10.94</b>

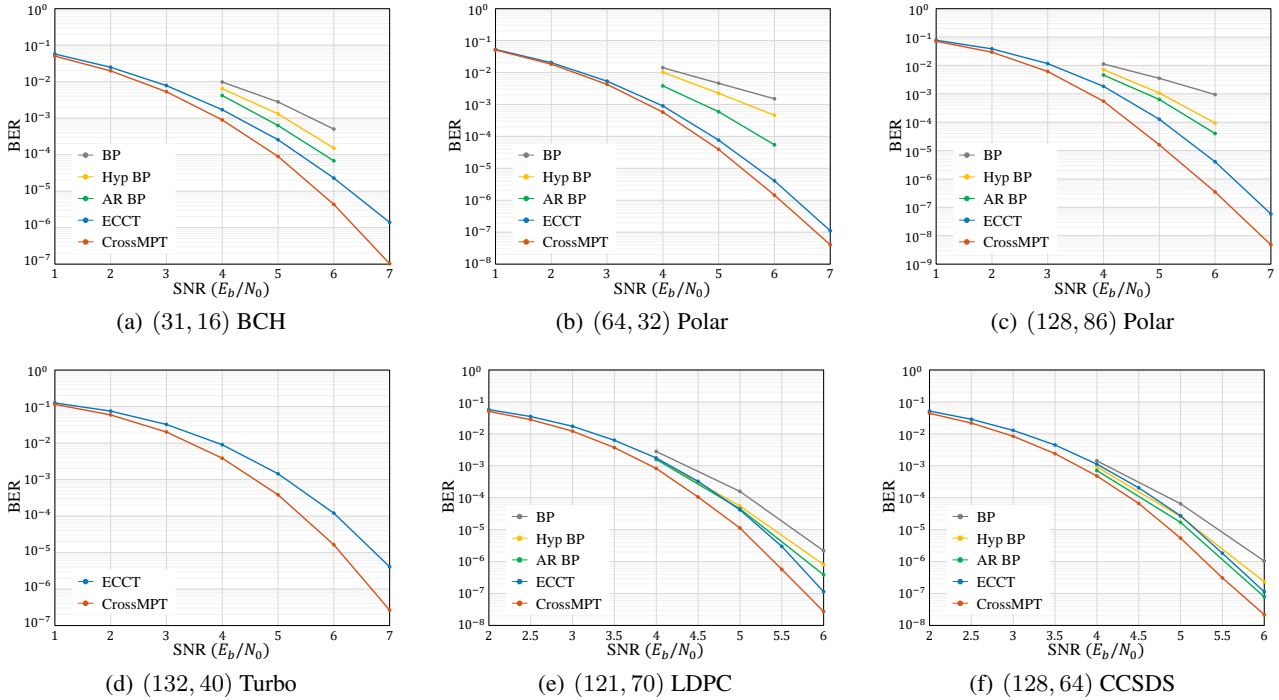


Figure 6. The BER performance of various decoders (BP, Hyp BP, AR BP, ECCT) and CrossMPT for (a) (31, 16) BCH code, (b) (64, 32) polar code, (c) (128, 86) polar code, (d) (132, 40) turbo code, (e) (121, 70) LDPC code, and (f) (128, 64) CCSDS.

## 5.2. Computational Complexity

Among all blocks in CrossMPT, the computational complexity of the attention module is the only part that differs from

the original ECCT. For the remaining parts, two architectures have the same computational complexity.

**ECCT architecture.** Let  $\tilde{y} = [|y|, s(y)]$  be the input embedding vector of the original ECCT, where  $|y|$  is the magnitude of  $y$  with the size  $1 \times n$  and  $s(y)$  is the syndrome of  $y$  with the size  $1 \times (n - k)$ . The projection matrices of  $\tilde{y}$  onto the query, key, and value are  $Q = \tilde{y}W_Q$ ,  $K = \tilde{y}W_K$ , and  $V = \tilde{y}W_V$ , respectively, where  $W_Q, W_K, W_V \in \mathbb{R}^{d \times d}$ . The computation of the attention mechanism is given by

$$\text{Attention}(Q, K, V) = \text{softmax} \left( \frac{QK^T}{\sqrt{d}} \right) V, \quad (2)$$

which is also known as the scaled dot-product attention.

Let  $C_1$  be the computational complexity of the self-attention mechanism of ECCT. According to (2),  $C_1$  is given by

$$\begin{aligned} C_1 &= (2n - k)^2 \times d + (2n - k)^2 + (2n - k)^2 \times d \\ &= 2(2n - k)^2 d + (2n - k)^2 \\ &= (2n - k)^2 (2d + 1). \end{aligned} \quad (3)$$

**CrossMPT architecture.** The input vectors of CrossMPT are  $|y|$  and  $s(y)$  and each is the query of two cross-attention modules. Let  $C_2$  be the computational complexity of the cross-attention mechanism of CrossMPT. According to (2),  $C_2$  is given as

$$\begin{aligned} C_2 &= 2 \times (n(n - k) \times d + n(n - k) + n(n - k) \times d) \\ &= 4n(n - k)d + 2n(n - k) \\ &= 2n(n - k)(2d + 1). \end{aligned} \quad (4)$$

**Computational complexity ratio.** The computational complexity ratio of the attention modules in the two architectures can be defined by  $\gamma = C_2/C_1$ , which is the computational complexity ratio of the attention modules and  $R$  be the code rate. Then, from (3) and (4),  $\gamma$  is given as

$$\begin{aligned} \gamma &= \frac{2n(n - k)(2d + 1)}{(2n - k)^2(2d + 1)} = \frac{2n(n - k)}{(2n - k)^2} = \frac{2n(n - Rn)}{(2n - Rn)^2} \\ &= \frac{2(1 - R)}{(2 - R)^2} < \frac{1}{2}, \end{aligned} \quad (5)$$

where  $0 < k < n$ .

Figure 8 presents the computational complexity ratio  $\gamma$  according to the code rate  $R$ . As shown in Figure 8, CrossMPT achieves a substantial reduction in the computational complexity of the attention module compared to the original ECCT by at least  $1/2$ . As the code rate increases, the reduction becomes more pronounced. Since the attention module

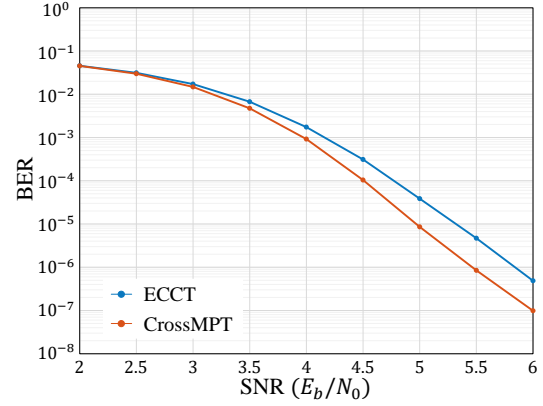


Figure 7. The BER performance of (384,320) WRAN for  $N = 6$  and  $d = 32$ .

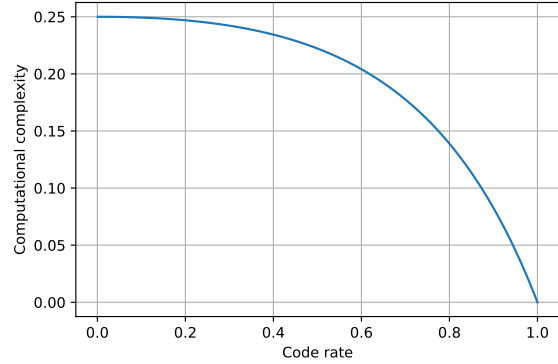


Figure 8. Computation complexity reduction according to the code rate.

constitutes a large proportion of the overall computational complexity, the benefits of CrossMPT are amplified as the neural network deepens.

Table 2 compares ECCT and CrossMPT training time for a single epoch. The training time is affected by parameters  $N$ ,  $d$ , and the codeword length. Under the same conditions, CrossMPT exhibits a significantly shorter training time compared to ECCT. A key metric in this table is *Time reduction*, which quantifies the training time reduction in percentage. As shown in (5), the ratio is closely associated with the code rate  $R$  and the number of decoder layers  $N$ . As  $R$  increases,  $\gamma$  becomes smaller while maintaining the computational complexity of the remaining layers, except for the attention module. Also, since CrossMPT achieves higher gain when the neural network becomes deeper, for the same  $R$ , *Time reduction* increases as  $N$  increases. The results in Table 1 and 2 demonstrate that the proposed CrossMPT not

Table 2. A training time comparison between ECCT and CrossMPT according to  $R$ ,  $N$ , and  $d$ . The training time is measured for a single epoch.

Code	$R = 5/6$			$R = 3/4$			$R = 1/2$		
	(648,540) LDPC	(648,540) LDPC	(384,320) WRAN	(576,432) WiMAX	(576,432) WiMAX	(384,288) WRAN	(96,48) MACKAY	(128,64) CCSDS	(384,192) WRAN
$(N, d)$	(2, 128)	(3, 128)	(6, 32)	(2, 128)	(3, 128)	(6, 32)	(2, 128)	(3, 128)	(6, 32)
ECCT	299 s	446 s	246 s	277 s	414 s	276 s	20 s	39 s	488 s
CrossMPT	111 s	165 s	86 s	126 s	188 s	112 s	17 s	28 s	239 s
Time reduction	62.93%	63.11%	65.04%	54.56%	54.62%	59.40%	15.00%	27.99%	50.96%

only outperforms the decoding performance but also highly reduces the training time compared to the original ECCT.

## 6. Conclusion

We developed a novel cross-attention message-passing transformer called CrossMPT, which aims to improve both decoding performance and reduce computational complexity. CrossMPT achieves this by facilitating the exchange of information between magnitude and syndrome vectors through the refined cross-attention mechanism, thereby improving the decoding performance. This approach, leveraging the PCM’s clear and compact definition of codeword bit relationships, empowers the model to accurately learn these well-defined relationships. Remarkably, CrossMPT outperforms ECCT across various codes, including BCH, polar, turbo, and LDPC codes. Especially for LDPC codes, CrossMPT significantly improves the decoding performance over ECCT by nearly 1 dB. Furthermore, CrossMPT achieves a reduction in the computational complexity of the attention module by at least 50%, compared to the original ECCT architecture.

## 7. Related Works

In the field of neural network-based ECC decoders, there are two primary categories: the model-based decoder and the model-free decoder.

**Model-based neural decoder.** First, model-based decoders are constructed based on the conventional decoding methods (e.g., BP decoder and MS decoder). They map the iterative decoding process of the conventional decoding methods into neural networks and train weights in neural networks. Although these model-based neural decoders guarantee the performance of underlying decoding methods, they might face performance limits due to the restrictive architecture being tightly bound to underlying decoding methods. Unlike the model-based decoders, the model-free neural decoders employ arbitrary neural network architectures to learn the decoding without prior knowledge of decoding algorithms.

To improve performance over the standard BP decoder, the recurrent neural network was utilized for decoding BCH codes (Nachmani et al., 2018). For the protograph LDPC codes, neural MS decoders with a parameter sharing technique have been proposed (Dai et al., 2021). Recently, the boost learning method for neural MS decoders (Kwak et al., 2023) was proposed to mitigate the error-floor phenomenon of LDPC codes. Furthermore, several studies showed that neural network-based BP and MS decoders improved the conventional decoders (Nachmani & Wolf, 2019; 2021; Kwak et al., 2022; Buchberger et al., 2021; Lugosch & Gross, 2017).

**Model-free neural decoder.** The preprocessing method utilizing the magnitude and syndrome vectors of the received codeword to learn multiplicative noise has been pivotal in enabling model-free decoders to address the overfitting issue (Bennatan et al., 2018). After this work, ECCT (Choukroun & Wolf, 2022a) first implemented the transformer architecture using the same preprocessing step and demonstrated that the ECCT outperforms the existing decoders including model-based neural decoders. Following the framework of ECCT, denoising diffusion error correction codes (Choukroun & Wolf, 2023) considered the decoding process as a diffusion process and employed diffusion model to the original ECCT architecture. Recently, double-masked ECCT (Park et al., 2023) utilized two different PCMs for the same linear code to capture the diverse features of the bit relationship and improve the decoding performance.

## References

- Bennatan, A., Choukroun, Y., and Kisilev, P. Deep learning for decoding of linear codes—a syndrome-based approach. In *Proceedings of 2018 IEEE International Symposium on Information Theory (ISIT)*, pp. 1595–1599. IEEE, 2018.
- Brown, T., Mann, B., Ryder, N., Subbiah, M., Kaplan, J. D., Dhariwal, P., Neelakantan, A., Shyam, P., Sastry, G., Askell, A., Agarwal, S., Herbert-Voss, A., Krueger, G., Henighan, T., Child, R., Ramesh, A., Ziegler, D., Wu, J.,

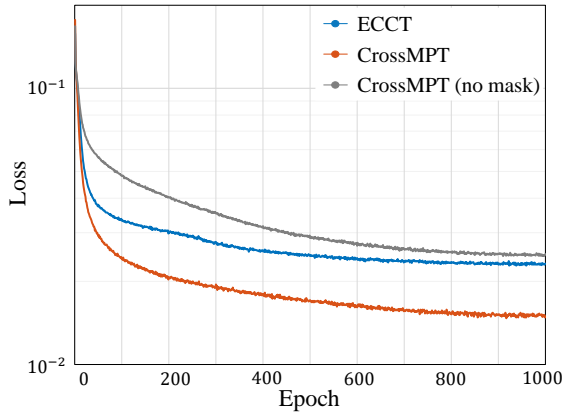


- Winter, C., Hesse, C., Chen, M., Sigler, E., Litwin, M., Gray, S., Chess, B., Clark, J., Berner, C., McCandlish, S., Radford, A., Sutskever, I., and Amodei, D. Language models are few-shot learners. In *Advances in Neural Information Processing Systems (NeurIPS)*, 2020.
- Buchberger, A., Hager, C., Pfister, H. D., Schmalen, L., and Amat, A. G. I. Pruning and quantizing neural belief propagation decoders. *IEEE Journal of Selected Areas in Communications*, 39(7):1957–1966, 2021.
- Carion, N., Massa, F., Synnaeve, G., Usunier, N., Kirillov, A., and Zagoruyko, S. End-to-end object detection with transformers. In *Proceedings of the European conference on computer vision (ECCV)*, 2020.
- Choukroun, Y. and Wolf, L. Error correction code transformer. In *Advances in Neural Information Processing Systems (NeurIPS)*, 2022a.
- Choukroun, Y. and Wolf, L. Error correction code transformer. <https://github.com/yoniLc/ECCT>, 2022b. Accessed: 2023-05-22.
- Choukroun, Y. and Wolf, L. Denoising diffusion error correction codes. In *Proceedings of International Conference on Learning Representations (ICLR)*, 2023.
- Dai, J., Tan, K., Si, Z., Niu, K., Chen, M., Poor, H. V., and Cui, S. Learning to decode protograph ldpc codes. *IEEE Journal of Selected Areas in Communications*, 39(7):1983–1999, 2021.
- Devlin, J., Chang, M.-W., Lee, K., and Toutanova, K. BERT: Pre-training of deep bidirectional transformers for language understanding. In *North American Chapter of the Association for Computational Linguistics (NAACL)*, 2019.
- Fossorier, M. P. C., Mihaljevic, M., and Imai, H. Reduced complexity iterative decoding of low-density parity check codes based on belief propagation. *IEEE Transactions on Communications*, 47(5):673–680, 1999.
- Girshick, R., Donahue, J., Darrell, T., and Malik, J. Rich feature hierarchies for accurate object detection and semantic segmentation. In *Proceedings of the IEEE/CVF Conference on Computer Vision and Pattern Recognition (CVPR)*, 2014.
- He, K., Gkioxari, G., Dollar, P., and Girshick, R. Mask R-CNN. In *Proceedings of the IEEE/CVF International Conference on Computer Vision (ICCV)*, 2015.
- He, K., Zhang, X., Ren, S., and Sun, J. Deep residual learning for image recognition. In *Proceedings of the IEEE/CVF Conference on Computer Vision and Pattern Recognition (CVPR)*, 2016.
- Helmling, M., Scholl, S., Gensheimer, F., Dietz, T., Kraft, D., Ruzika, S., and Wehn, N. Database of Channel Codes and ML Simulation Results. In <https://rptu.de/en/channel-codes>, 2019.
- Kim, H., Jiang, Y., Rana, R., Kannan, S., Oh, S., and Viswanath, P. Communication algorithms via deep learning. In *International Conference on Learning Representations (ICLR)*, 2018.
- Kim, H., Oh, S., and Viswanath, P. Physical layer communication via deep learning. *IEEE Journal of Selected Topics in Information Theory*, 1(1):5–18, 2020.
- Kingma, D. P. and Ba, J. Adam: A method for stochastic optimization. In *arXiv preprint arXiv:1412.6980*, 2014.
- Krizhevsky, A., Sutskever, I., and Hinton, G. E. ImageNet classification with deep convolutional neural networks. In *Advances in Neural Information Processing Systems (NeurIPS)*, 2012.
- Kwak, H.-Y., Kim, J.-W., Kim, Y., Kim, S.-H., and No, J.-S. Neural min-sum decoding for generalized ldpc codes. *IEEE Communications Letters*, 26(12):2841–2845, 2022.
- Kwak, H.-Y., Yun, D.-Y. and Kim, Y., Kim, S.-H., and No, J.-S. Boosting Learning for LDPC Codes to Improve the Error-Floor Performance. In *Advances in Neural Information Processing Systems (NeurIPS)*, 2023.
- Lugosch, L. and Gross, W. J. Neural offset min-sum decoding. In *Proceedings of 2017 IEEE International Symposium on Information Theory (ISIT)*, pp. 1316–1365. IEEE, 2017.
- Nachmani, E. and Wolf, L. Hyper-graph-network decoders for block codes. In *Advances in Neural Information Processing Systems (NeurIPS)*, pp. 2326–2336, 2019.
- Nachmani, E. and Wolf, L. Autoregressive belief propagation for decoding block codes. In *arxiv preprint arXiv:2103.11780*, 2021.
- Nachmani, E., Beery, Y., and Burshtein, D. Learning to decode linear codes using deep learning. In *2016 54th Annual Allerton Conference on Communications, Control, and Computing (Allerton)*, pp. 341–346. IEEE, 2016.
- Nachmani, E., Marciano, E., Lugosch, L., Gross, W. J., Burshtein, D., and Beery, Y. Deep learning methods for improved decoding of linear codes. *IEEE Journal of Selected Topics in Signal Processing*, 12(1):119–131, 2018.
- Park, S.-J., Kwak, H.-Y., Kim, S.-H., Kim, S., Kim, Y., and No, J.-S. How to mask in Error Correction Code Transformer: Systematic and double masking. In *arXiv preprint arXiv:2308.08128*, 2023.

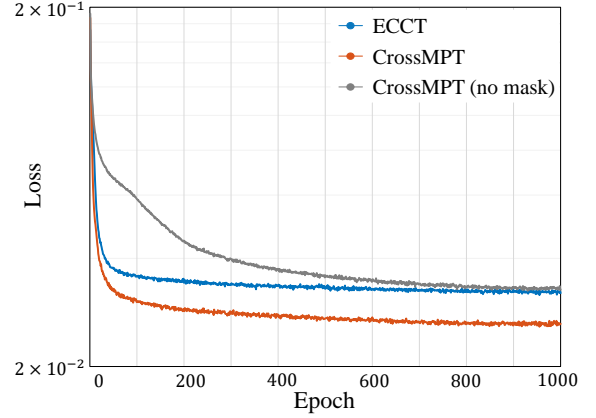
- 
- Redmon, J., Divvala, S., Girshick, R., and Farhadi, A. You only look once: Unified, real-time object detection. In *Proceedings of the IEEE/CVF Conference on Computer Vision and Pattern Recognition (CVPR)*, 2015.
- Ren, S., He, K., Girshick, R., and Sun, J. Faster R-CNN: Towards real-time object detection with region proposal networks. In *Advances in Neural Information Processing Systems (NeurIPS)*, 2015.
- Richardson, T. and Urbanke, R. The capacity of low-density parity check codes under message-passing decoding. *IEEE Transactions on Information Theory*, 47 (2):599–618, 2001.
- Simonyan, K. and Zisserman, A. Very deep convolutional networks for large-scale image recognition. In *Proceedings of International Conference on Learning Representations (ICLR)*, 2015.
- Szegedy, C., Liu, W., Jia, Y., Sermanet, P., Reed, S., Anguelov, D., Erhan, D., Vanhoucke, V., and Rabinovich, A. Going deeper with convolutions. In *Proceedings of the IEEE/CVF Conference on Computer Vision and Pattern Recognition (CVPR)*, 2015.

## A. Impact of the Proposed Mask Matrix and Training Convergence

The mask matrix in transformer-based decoders enables the model to efficiently learn the relevance between codeword bits. In the masked cross-attention module in CrossMPT, the mask matrix is the PCM itself, utilizing only the essential information of codeword bits. To demonstrate the impact of the mask matrix in CrossMPT, we measure the loss for each iteration. Figure 9 compares the training convergence between ECCT, CrossMPT, and CrossMPT with no masking. CrossMPT with no masking has worse training convergence compared to ECCT architecture. Also, for iterations less than 300 in (121,70) LDPC codes, the graph shows that CrossMPT with no masking encounters difficulty in learning to estimate transmitted codeword. As shown in the figure, the benefit of utilizing a mask matrix in CrossMPT architecture is straightforward.



(a) Polar (128, 86)



(b) LDPC (121, 70)

Figure 9. The loss at each epoch for (a) (128,86) polar code and (b) (121,70) LDPC code.

## B. Performance on Larger Codes

We present the BER graph for larger codes in Figure 10 for ECCT and CrossMPT  $N = 6, d = 32$ . As shown in the figure, CrossMPT still performs well for codeword lengths larger than 500. For (529,440) LDPC codes and (512,384) polar codes, the proposed CrossMPT outperforms the original ECCT.

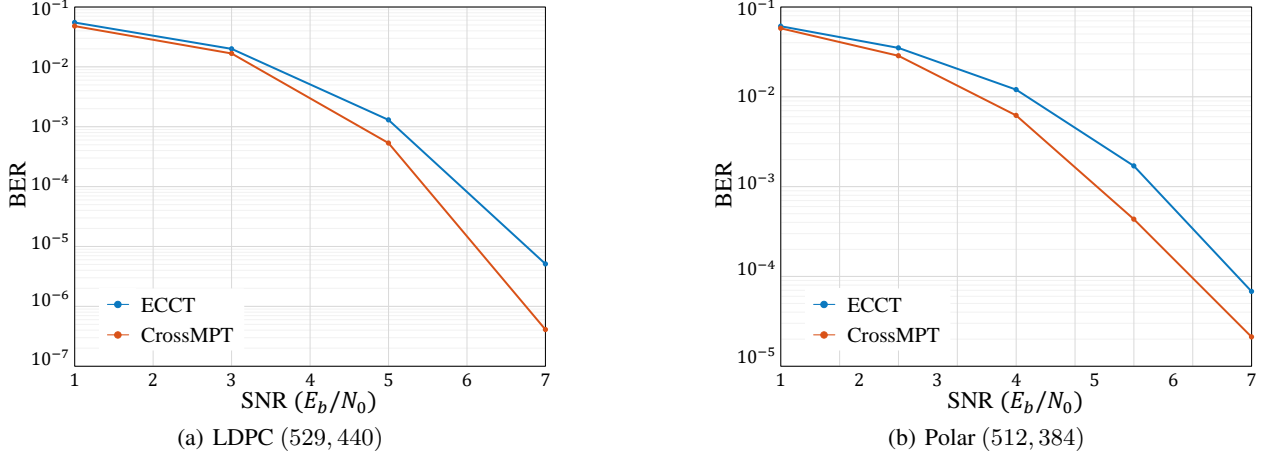


Figure 10. The decoding performance comparison between ECCT, DDECC, and CrossMPT  $N = 6, d = 32$  for (a) (529,440) LDPC codes and (b) (512,384) polar codes.

Also, Figure 11 shows the decoding performance of CrossMPT for much larger codes. The BER performance of the (648,540) IEEE802.11n LDPC code demonstrates that CrossMPT efficiently trains how to decode the codeword even for large  $N$  and  $d$  and performs well for larger codes. In contrast to CrossMPT, which highly reduces the computational complexity compared to ECCT, ECCT cannot train codewords longer than 1000 within the same training environment. The BER performance of the (1056,880) WiMAX LDPC code demonstrates that CrossMPT performs well even for codeword lengths larger than 1000.

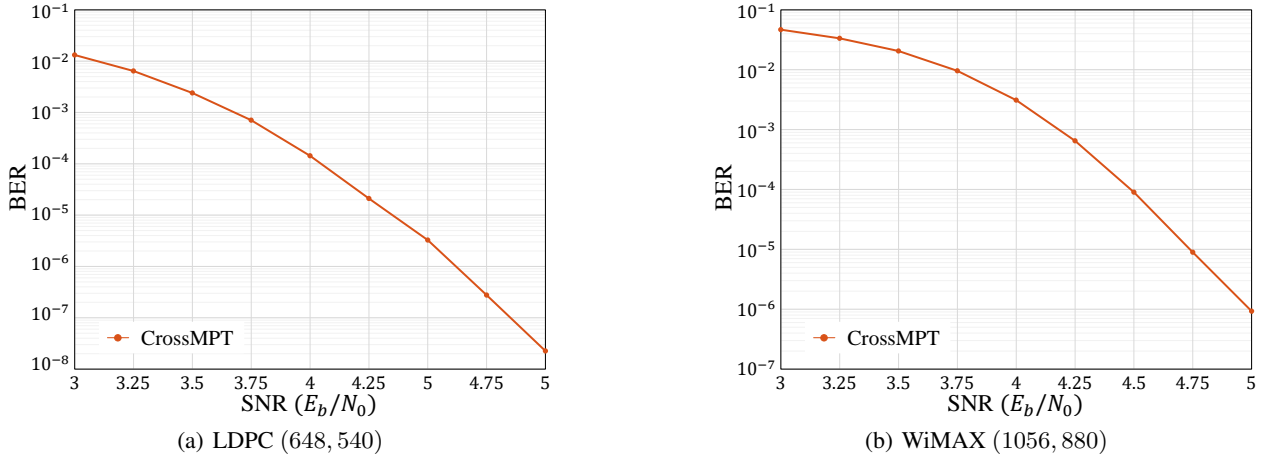


Figure 11. The decoding performance of CrossMPT. (a) (648,540) IEEE802.11n LDPC code for  $N = 10, d = 128$  and (b) (1056,880) WiMAX LDPC code for  $N = 6, d = 32$ .

## C. Comparison with ECCT Architectures

Table 3 compares the BER performance of vanilla transformer-based decoders (ECCT (Choukroun & Wolf, 2022a) and CrossMPT) and denoising diffusion error correction code (DDECC (Choukroun & Wolf, 2023)). All three works are model-free decoders using transformer architecture, and simulations are taken for  $N = 6$ ,  $d = 128$ . Compared to the original ECCT, a vanilla transformer-based decoder like ours, our work shows a superior decoding performance. Compared to DDECC, CrossMPT demonstrates similar BER performance in polar codes, but it even outperforms DDECC in BCH and LDPC codes. It is worth noting that the diffusion model can also be adapted to CrossMPT architecture. Since CrossMPT architecture achieves better decoding performance and computational complexity than the original ECCT architecture, it has a strong potential when the diffusion model is added to CrossMPT architecture.

Table 3. A comparison of decoding performance at three different SNR values (4 dB, 5 dB, 6 dB) for ECCT (Choukroun & Wolf, 2022a), CrossMPT, and DDECC (Choukroun & Wolf, 2023). The results are measured by the negative natural logarithm of BER. The best results are highlighted in **bold**. Higher is better.

Architecture		Vanilla transformer-based decoder						Diffusion model + ECCT		
Codes	Method	ECCT			CrossMPT			DDECC		
		4	5	6	4	5	6	4	5	6
BCH	(63,36)	4.86	6.65	9.10	5.03	6.91	9.37	<b>5.11</b>	<b>7.09</b>	<b>9.82</b>
	(63,45)	5.60	7.79	10.93	<b>5.90</b>	<b>8.20</b>	<b>11.62</b>	5.61	7.94	11.36
	(63,51)	5.66	7.89	11.01	<b>5.78</b>	<b>8.08</b>	<b>11.41</b>	5.26	7.40	10.49
Polar	(64,32)	6.99	9.44	12.32	<b>7.50</b>	<b>9.97</b>	<b>13.31</b>	6.93	9.51	12.79
	(64,48)	6.36	8.46	11.09	<b>6.51</b>	<b>8.70</b>	<b>11.31</b>	5.96	8.04	10.98
	(128,64)	5.92	8.64	12.18	7.52	11.21	14.76	<b>9.11</b>	<b>12.9</b>	<b>16.30</b>
	(128,86)	6.31	9.01	12.45	7.51	<b>10.83</b>	<b>15.24</b>	<b>7.60</b>	10.81	15.17
	(128,96)	6.31	9.12	12.47	7.15	10.15	13.13	<b>7.16</b>	<b>10.3</b>	<b>13.19</b>
LDPC	(49,24)	6.13	8.71	12.10	<b>6.68</b>	<b>9.52</b>	<b>13.19</b>	5.88	8.27	11.42
	(121,60)	5.17	8.31	13.30	<b>5.74</b>	<b>9.26</b>	<b>14.78</b>	5.38	8.73	14.17
	(121,70)	6.40	10.21	16.11	<b>7.06</b>	<b>11.39</b>	<b>17.52</b>	6.79	11.13	16.93
	(121,80)	7.41	11.51	16.44	<b>7.99</b>	<b>12.75</b>	<b>18.15</b>	7.59	12.17	16.89
Mackay	(96,48)	7.38	10.72	14.83	7.97	11.77	15.52	<b>8.12</b>	<b>11.88</b>	<b>15.93</b>
CCSDS	(128,64)	6.88	10.90	15.90	<b>7.68</b>	11.88	17.50	7.27	<b>12.48</b>	<b>17.66</b>